Simulation of Thermal Dependence of MR signal on Slider Flying State

Li Chen, Xinjiang Shen and David B. Bogy

Computer Mechanics Laboratory, University of California at Berkeley
5146 Etcherverry Hall, Berkeley, CA, 94706
Tel.: 510-64249. Fax: 510-6439786

ABSTRACT

In this report, we summarize our simulation work on the thermal dependence of the MR signal on the slider flying state and provide a user manual for the related programs. Some new simulation results are also presented. In the simulation we used a three dimensional (3-D) heat transfer model for the slider body. The simulation work includes two parts: a) the static thermal simulation that combines with the CML Air Bearing Design Program to obtain the steady state MR signal dependence on the slider flying state; b) the dynamic thermal simulation that is used with the CML Dynamic Simulator to study the dynamic response of the MR signal when the slider flies over a bump, with or without contact.

Keywords: MR sensor, MR element, thermal asperity, static thermal simulation, dynamic thermal simulation.

1. Introduction

Since the electrical resistance of the MR sensor is temperature dependent, the read-back signal of a magneto-resistive (MR) head can be significantly affected by thermal influences. This thermal influence comes mainly from the heat flux between the disk and the MR sensor. It also depends on the MR structure and the flying state of the slider. There have recently been several studies of the heat transfer mechanism related to MR read-back signal disturbances in hard disk drives at the Computer Mechanics Laboratory at the University of California at Berkeley. Zhang and Bogy (1997) studied the heat transfer between the slider and the air bearing, and they also developed a 2-D heat conduction model for the slider body (1998)a.

Chen and Bogy (1999) developed a 3-D heat transfer model in the slider body. The expression of the heat flux between the slider and air bearing film was also modified from Zhang and Bogy (1997). This reportis based o n the Chen and Bogy (1999) report. It serves as a user manual for all of the thermal simulations of the MR signal. The thermal simulation includes two parts: a static part and a dynamic part. The thermal programs in both parts work together with some other CML software package. For the static thermal simulation, the CML Air bearing Design Program is used to obtain the static pressure and spacing in the air bearing given an initial virtual flying height at the central trailing edge, slider pitch and roll. And then the static pressure and spacing in the air bearing are used as input to the dynamic thermal simulation. For the dynamic thermal simulation, the thermal part has been included in the CML Dynamic Simulator as subroutines. The CML Dynamic Simulator calls these subroutines at each time step. Using the values calculated by the CML Dynamic Simulator such as, contact pressure, local pressure in the air bearing and flying height, the thermal subroutine performs the simulation when the slider flies over as asperity, with or without contact. Some of these results will be shown in this report. First we recall the theoretical developments of our previous reports on this topic.

2. Heat Flux from Slider to Air Bearing

For a MR sensor embedded in a slider, the signals will change due to temperature change; the governing equation for heat transfer is:

$$\rho c \frac{\partial T}{\partial \tau} = \frac{\partial}{\partial x}\left(k \frac{\partial T}{\partial x}\right) + \frac{\partial}{\partial y}\left(k \frac{\partial T}{\partial y}\right) + \frac{\partial}{\partial z}\left(k \frac{\partial T}{\partial z}\right) + S \tag{1}$$

where

$$S = \begin{cases} Q_0 = \dfrac{I_s^2 R_s}{V_s} & for \quad (x, y, x) \in \Gamma_{MR} \\ 0 & for \quad (x, y, x) \notin \Gamma_{MR} \end{cases} \tag{2}$$

in which Γ_{MR} is the region occupied by the MR sensor. Due to the cooling effects of the air bearing film, the boundary conditions for the slider can be divided to two parts: First, the heat exchange between the slider and the ambient environment can be described as

$$q = h_C (T - T_0). \tag{3}$$

Second, the heat flux between the slider and the air bearing has to be calculated from the energy equation,

$$\rho_a C_{p_a} u \frac{\partial T}{\partial x} + \rho_a C_{p_a} u \frac{\partial T}{\partial y} - u \frac{\partial p}{\partial x} - u \frac{\partial p}{\partial y} = \frac{\partial}{\partial z}\left(k_a \frac{\partial T}{\partial z}\right) + \mu_a \left(\frac{\partial u}{\partial z}\right)^2 + \mu_a \left(\frac{\partial v}{\partial z}\right)^2 \tag{4}$$

where ρ_a is the air densiy, c_{pa} is the air specific heat, k_a is the air thermal conductivity. T, p, u, v are temperature, pressure and velocity components of the air bearing film, respectively. The boundary conditions for air bearing are (Zhang and Bogy (1997)):

z=0 (Rotating disk surface)

$$T(0) = T_d + 2\frac{2-\sigma_T}{\sigma_T}\frac{\gamma}{\gamma+1}\frac{\lambda}{\Pr}\frac{\partial T}{\partial z}\Big|_{z=0} \tag{5}$$

$$u(0) = U + \frac{2-\sigma_M}{\sigma_M}\lambda\frac{\partial u}{\partial z}\Big|_{z=0} \tag{6}$$

$$v(0) = \frac{2-\sigma_M}{\sigma_M}\lambda\frac{\partial v}{\partial z}\Big|_{z=0} \tag{7}$$

z=h (Slider surface)

$$T(h) = T_s - 2\frac{2-\sigma_T}{\sigma_T}\frac{\gamma+1}{\gamma}\frac{\lambda}{\Pr}\frac{\partial T}{\partial z}\Big|_{z=h} \tag{8}$$

$$u(h) = -\frac{2-\sigma_M}{\sigma_M}\lambda\frac{\partial u}{\partial z}\Big|_{z=h} \tag{9}$$

$$v(h) = -\frac{2-\sigma_M}{\sigma_M}\lambda\frac{\partial v}{\partial z}\Big|_{z=h} \tag{10}$$

where σ_M is the momentum accommodation coefficient; σ_T is the thermal accommodation coefficient; γ is the ratio of specific heats at constant pressure and constant volume; λ is the mean-free-path of the air and h is the air bearing spacing.

From Zhang and Bogy (1997), we also have

$$u = -\frac{1}{2\mu_a}\frac{\partial p}{\partial x}\left(a\lambda h + hz - z^2\right) + U\left(1 - \frac{z + a\lambda}{h + 2a\lambda}\right) \tag{11}$$

$$v = -\frac{1}{2\mu_a}\frac{\partial p}{\partial y}\left(a\lambda h + hz - z^2\right) \tag{12}$$

Therefore,

$$\frac{\partial u}{\partial z} = -\frac{1}{2\mu_a}\frac{\partial p}{\partial x}\left(h - 2z\right) - U\frac{1}{h + 2a\lambda} \tag{13}$$

$$\frac{\partial v}{\partial z} = -\frac{1}{2\mu_a}\frac{\partial p}{\partial y}(h-2z). \tag{14}$$

Substituting (13) and (14) into the simplified energy equation,

$$-u\frac{\partial p}{\partial x} - v\frac{\partial p}{\partial y} = \frac{\partial}{\partial z}\left(k_a \frac{\partial T}{\partial z}\right) + \mu_a\left(\frac{\partial u}{\partial z}\right)^2 + \mu_a\left(\frac{\partial v}{\partial z}\right)^2, \tag{15}$$

we obtain

$$\begin{aligned}\frac{\partial}{\partial z}\left(k_a \frac{\partial T}{\partial z}\right) = &\left[\frac{1}{2\mu_a}\frac{\partial p}{\partial x}\left(a\lambda h + hz - z^2\right) - U\left(1 - \frac{z + a\lambda}{h + 2a\lambda}\right)\right]\frac{\partial p}{\partial x} \\ &+ \frac{1}{2\mu_a}\left(\frac{\partial p}{\partial y}\right)^2\left(a\lambda h + hz - z^2\right) - \mu_a\left[\left(\frac{\partial u}{\partial z}\right)^2 + \left(\frac{\partial v}{\partial z}\right)^2\right].\end{aligned} \tag{16}$$

The temperatures at the disk and slider surfaces are denoted as T_d and T_s, respectively, that is,

$$T\big|_{z=0} = T_d,$$

$$T\big|_{z=h} = T_s. \tag{17}$$

Fourier's law, $q = -k_a \frac{\partial T}{\partial z}\Big|_{z=h}$ is used to calculate the heat flux, which we divide into two parts,

$$q = q_{Zhangsy} + q_{PG}, \tag{18}$$

where

$$\begin{aligned}q_{Zhangsy} = &-k_a\frac{T_s - T_d}{h + 2b\lambda} + \frac{h^3}{24\mu_a}\left[\left(\frac{\partial p}{\partial x}\right)^2 + \left(\frac{\partial p}{\partial y}\right)^2\right] + \frac{\mu_a U^2 h}{2(h + 2a\lambda)^2} \\ &- \frac{Uh^3}{6(h + 2b\lambda)(h + 2a\lambda)}\frac{\partial p}{\partial x},\end{aligned} \tag{19}$$

and

$$q_{PG} = -\frac{h^2}{24\mu_a}(6a\lambda + h)\left[\left(\frac{\partial p}{\partial x}\right)^2 + \left(\frac{\partial p}{\partial y}\right)^2\right] + \frac{Uh}{2}\left(\frac{a\lambda + \frac{h}{3}}{2a\lambda + h}\right)\frac{\partial p}{\partial x} \tag{20}$$

where $a = \frac{2-\sigma_M}{\sigma_M}$ and $b = \frac{2(2-\sigma_T)\gamma}{\sigma_T(\gamma+1)\mathrm{Pr}}$.

Therefore,

$$q = -k_a \frac{T_s - T_d}{h + 2b\lambda} - \frac{a\lambda h^2}{4\mu_a}\left[\left(\frac{\partial p}{\partial x}\right)^2 + \left(\frac{\partial p}{\partial y}\right)^2\right] + \frac{\mu_a U^2 h}{2(h + 2a\lambda)^2}$$

$$+ \frac{Uh\left[3ah\lambda + 2bh\lambda + 6ab\lambda^2\right]}{6(h + 2a\lambda)(h + 2b\lambda)}\frac{\partial p}{\partial x}. \tag{21}$$

For ultra thin air bearing films, the mean free path of airs changes with pressure, Guthrie and wakerling (1949),

$$\lambda = \lambda_0 \frac{p_0}{p} \tag{22}$$

where p is the local instantaneous pressure and λ_0 is the mean free path at ambient pressure p_0.

Previously, Chen and Bogy (1999) derived the heat flux between the slider and air bearing film as:

$$q = -k_a \frac{T_s - T_d}{h + 2b\lambda_0 \frac{p_0}{p}} - \frac{a\lambda_0 p_0 h^2}{4p\mu_a}\left[\left(\frac{\partial p}{\partial x}\right)^2 + \left(\frac{\partial p}{\partial y}\right)^2\right] + \frac{\mu_a U^2 h}{2\left(h + 2a\lambda_0 \frac{p_0}{p}\right)^2}$$

$$+ \frac{Uh\left[ah\lambda_0 \frac{p_0}{p} + bh\lambda_0 \frac{p_0}{p} + 2ab\left(\lambda_0 \frac{p_0}{p}\right)^2\right]}{6\left(h + 2b\lambda_0 \frac{p_0}{p}\right)\left(h + 2a\lambda_0 \frac{p_0}{p}\right)}\frac{\partial p}{\partial x} \tag{23}$$

which has a different and evidently incorrect last term than Eq. (21). We make that correction here and note that the term $\frac{Uh\left[3ah\lambda+2bh\lambda+6ab\lambda^2\right]}{6(h+2a\lambda)(h+2b\lambda)}\frac{\partial p}{\partial x}$ is 2 orders of magnitude smaller than $k_a\frac{T_s-T_d}{h+2b\lambda}$, this change of heat flux has little effect on the final numerical results. Therefore, the previous numerical results are still valid for the cases presented in the CML report 99-026.

3. Static Thermal Simulation

3.1 Input files

3.1.1 Input file *unstead1.dat.*

```
********************** input file Unstead1.dat ***********************
**********************Geometry of Slider******************************
xsl          ysl          ysh          zsh     thick   x_mr         y_mr    z_mr
2.012d-3     1.39d-3      1.42d-3      80d-6   0.3d-3  0.05d-06     6.d-6   1.7d-6
MR        W_shield  W_top     w_gap1   W_gap2   W_gap3
0.05d-06  4.d-06    5.d-06    0.4d-06  0.1d 06  0.1d-06
****************Electrical Properties and Grid options*********************
bias_I       R_zero   npx    npy
1.25d-2      25.d0    200    200
nx     ny     nz
80     80     40
nx_mr   nx_gap1   nx_gap2   nx_gap3   nx_shid   nx_top
5       2         5         5         10        5
ny_B_Shild    ny_shild    ny_B_MR    ny_MR
25            20          30         10
coat_h    nz_c    nz_mr    nzs
7.5d-09   2       12       25
***************Heat Transfer Properties*******************************
amu          lamda        Pr       Avogadro's number    p0
1.488e-5     0.635e-7     0.7d0    288.d0               1.0135e+5
kh      rouh         cph     ks      rous    cps     ka           sigma
1.01d0  4000.d0      600.d0  35.3d0  8.d3    460.d0  2.624d-2     0.9d0
gama    alfa
1.4d0   0.9d0
t0      tw      dt      tmax
300.d0  300.d0  1.d-6   6.d-4
****************Allowable Error for Heat Transfer Solver******************
Eps
```

1.0e-6

rail_key	save_key	read_key
1	0	1
xsl(ct.)	ysl	ysh
1.98e-3	0.785d-3	0.815d-3

************************* End of Input Data *************************

xsl: starting x-position of MR sensor (not normalized) [m]. Ending x-position of MR sensor is determined in subroutine Grid.

ysl: starting y-position of MR sensor (not normalized) [m].

ysh: ending y-position of MR sensor [m].

zsh: the height of MR sensor in z-direction [m].

thick: thickness of the slider in z-direction [m].

x_mr: size of the MR element in x-direction [m].

y_mr: size of the MR element in y-direction [m].

z_mr: size of the MR element in z direction [m].

MR: width of MR element[m].

W_shield: thickness of MR element shield[m].

W_top: width of top pole[m].

W_gap1, W_gap2, W_gap3:

widths of gap1, gap2 and gap3 in the MR sensor.

bias_I: bias current in MR sensor [A].

R_zero: initial electrical resistance of MR sensor [ohm].

npx: maximum grid size in x direction.

npy: maximum grid size in y direction.

nx,ny,nz: grid number for the air bearing film in x, y, z directions.

nx_mr, nx_gap1,nx_gap2,nx_gap3,nx_shid ,nx_top :

grid numbers for MR, gap1,gap2, gap3, shield and top pole in x direction.

ny_B_Shild,ny_shild ,ny_B_MR ,ny_MR :

grid numbers for the portions before shield and MR, shield and MR in y direction.

coat_h,nz_c,nz_mr,nzs :

	thickness of MR coating, grid sizes of coating, MR element and MR sensor in z direction.
amu:	viscosity of air [m2/s].
lamda:	mean free path of ambient air [m].
pr:	Prandtl number.
p0:	ambient pressure [N/ m2].
kh:	heat conductivity of the material around the MR sensor (w/m.k).
rouh:	density of the material around the MR sensor (kg/m3).
cph:	specific heat of the material around the MR sensor (J/kg.K).
ks:	heat conductivity of the MR sensor (w/m.k).
rous:	density of the MR sensor (kg/m3).
cps:	specific heat of the MR sensor (J/kg.K).
ka:	heat conductivity of the air (w/m.k).
sigma:	momentum accommodation coefficient.
gama:	ratio of specific heat at constant pressure and specific heat at constant volume.
alfa:	thermal accommodation coefficient.
t0:	initial slider surface temperature (k).
tw:	disk surface temperature (k).
dt, tmax:	time step and total time duration of the simulation (s).
Eps:	Allowed maximum error for temperature field.
rail_key:	1 = center rail and reading xsl, ysl, ysh from the last line;
	2 = non-center rail and not reading xsl, ysl, ysh on the last line.
save_key:	1 = saving the 3-d steady state temperature field of the slider to the output file sta_temp.dat.
	0 = not saving temperature.
read_key:	1 = reading the initial temperature from sta_temp.dat.
	0 = not reading the initial temperature from sta_temp.dat.

3.1.2 Other input files.

Other input files are *x.dat*, *y.dat*, *run.dat*, *rail.dat*, *results418.dat*, *press01.dat*, and *heigh01.dat*. The first two files are the input files for the CML Air Bearing Design Program, and they are in **quick400** format; *x.dat*, *y.dat*, *results418.dat*, *press01.dat* and *heigh01.dat* are the output files of the CML Air Bearing Design Program using the modified Quick 418 solver. *Press01.dat and heigh01.dat* are the 2-d pressure field and spacing data in the air bearing film for each grid.

Since the CML Air Bearing Design Program couldn't output the flying height at every grid, two of the source codes are modified somewhat. And the modified package is in directory */Quick_mod/quick418_mod/.* The construction of the whole package is the same as the quick4.18 version. The two source codes, which are modified and renamed, are: *inv.f* → *invht.f*, and *quick.f* → *quickh.f*. And this is also shown in the source codes list in the *makefile*. There are also comments in the modified source codes about these related changes. The compiled file, which can be run directly, is called *quickn*.

3.2 Output files.

The output files are: *sta_temp.dat* and *temp_res.dat*. The file *sta_temp.dat* is the 3-d temperature field in the slider body. And *temp_res.dat* is the output of gap spacing, gap temperature, gap pressure (normalized by ambient pressure), and disk velocity at the radius of the slider location. There is also a subroutine *heatflux* which can be used to output the heat flux in the air bearing when necessary.

3.3 How to run the main program

The goal of the static thermal program is to obtain the temperature inside the MR sensor under a static flying condition: flying height, pitch angle, skew angle, etc. In order to accomplish this, we need to know the pressure field and spacing in the air bearing under those conditions. So first run the CML Air Bearing Design Program to get the flying height results *results418.dat*, the pressure file *press01.dat* and spacing file *heigh01.dat*, as well as the *x* and *y* grid files *x.dat*, *y.dat*. Then copy these files to the directory where the thermal program will be running. Please use the modified CML Air Bearing Design Program in */Quick_mod/quick418_mod/* if the newest version can not output the spacing in the air bearing for every grid. As to how to run the CML Air Bearing Design Program, please refer to the manual (Lu and Bogy, 1995).

The source code of the static thermal program is *ht3d_sta.f*. It's in directory */Thm_3d_sta*/. All the subroutines are listed in Section 5.

Some simulation results have been obtained using the static thermal program. All the details are in CML Technical Report No. *99-026*.

4. Dynamic Thermal Simulation

4.1 Input files.

The input files are *unstead1.dat*, *rail.dat* and *dynamics.def*.

The file *unstead1.dat* is the same as for the static thermal simulation, while the file *rail.dat* is in **quick300** format. There is also manual for it (Hu and Bogy, 1995). The file *dynamics.def* is the input file for the CML Air Bearing Dynamic Simulator. For different cases of study, the values of some of the variables in *dynamics.def* should be changed.

4.2 Output files.

Output files are: *sta_temp.dat* and *temp_res.dat*. The file *sta_temp.dat* stores the 3-d temperature field in the slider body. This *sta_temp.dat* is the steady state temperature under the initial flying state. The *temp_res.dat* contains the slider response history at the MR sensor. There are eight columns of data: time (s) in column 1, gap temperature (C) in column 2, gap spacing (m) in column 3, gap pressure (normalized by ambient pressure) in column 4, average contact pressure in column 5, maximum contact pressure in column 6, x position of maximum contact pressure in column7, y position of maximum contact pressure in column 8.

4.3 Examples of Dynamic Thermal Simulation

The source file for dynamic simulation is *ht3d_dyn.f*. It's in directory */Thm_3d_dyn*/.

4.3.1. Dynamic MR temperature response for the slider flying over an asperity without contact (baseline wander).

In order to get the accurate initial flying condition for a specific rail shape, first, run the CML Air Bearing Design Program once to obtain a rough steady state flying condition such as flying height at the central trailing edge, pitch and roll. Then use these data as the initial flying condition in the input file *dynamics.def*. The corresponding variable names in the *dynamics.def* are *hm, hp,* and *hr*. Set other variables in the *dynamics.def* as in the following sample (note nasper = 0), so that steady conditions will be reached after the simulation has run long enough. There is an efficient way to do this:

run the CML Dynamic Simulator while setting the time duration *tf* to be about 0.5 ms; obtain the *hm*, *hp* and *hr* again from the output file *fhhist.dat* and change the initial condition in the *dynamics.def* according to these data; run the CML Dynamic Simulator and repeat the above steps a few times.

```
********************** Input file dynamics.def ******************
xl(m)          yl(/xl)        xg(/xl)        yg(/xl)        zg(/xl)        halt
0.2e-2         0.8            0.5            0.0            0.1075         0.0
 f0(kg)        xf0(xl)        yf0(/yl)       amz            aip            air
0.35e-2        0.5            0.0            0.59e-5        0.217e-11      0.136e-11
 rpm           dt(s)          tf(s)          ra             ra_if          ra_of
 6400.0        1.e-6          0.0005         23.0e-3        10.0e-3        50.0e-3
************************Suspension************************
iact           xact(m)        dact           vact           ske            xfs
1              38.00e-3       0.0            0.0            0.0            0.0
 isusp         nmodes         ncg            alfa           beta           yfs
0              10             2149           60.0           1.0e-5         0.0
skz            skp            skr            scz            scp            scr
21.22047       0.1037e-3      0.11058e-3     0.002          0.1579e-7      0.1396e-7
 *****************Initial Flying Condition****************
hm(m)          hp(rad)        hr(rad)        vz(m/s)        vp(rad/s)      vr(rad/s)
0.392464e-7    0.183299e-3    0.477018e-5    0.0            0.0            0.0
******************Solution Control***********************
 iqpo          akmax          emax            idisc
5              1.0e-10        1.0e-4         1
*******************Grid Control**************************
iadapt         isymmetry      ioldgrid       nx             ny             nsx    nsy
0              0              1              193            193            1      1
xnt(i),i=2,nsx
0.0
nxt(i),i=2,nsx
0
dxr(i),i=1,nsx
1.0
ynt(i),i=2,nsy
0.0
nyt(i),i=2,nsy
0
dyr(i),i=1,nsy
1.000000
difmax         decay           ipmax
40.0            40.0           0
***********Point by Point Disk Track Profile**************
```

```
ims             nfx             dinit
0               1009            3.2
******Numerical Generation of Disk Surface Topography******
nwave           nzone           nasper
0               0               0
iwtype          wamp(m) wang(dg) wthx(m) wthy(m) wpdx(m) wpdy(m) wrs(m) wre(m)
zr1(m)          zh1(m)          zr2(m)          zh2(m)          zr3(m)          zh3(m)
iatype          aamp(m)         aang(dg)        alocx(m) alocy(m)  asizx(m)  asizy(m)
****Numerical Generation of Slider Surface Topography******
nswave          nsasper
0               0
istype  swamp(m)  swng(dg)  swthx(m)   swthy(m)   swpdx(m)   swpdy(m)
isatype saamp(m)  saang(dg) salocx(m)  salocy(m)  sasizx(m)  sasizy(m)
******************Track Accessing Motion*******************
nap
0
tac(s)          aac(rad/s^2)
*************Time-Dependent Disk Velocity*****************
nvp
0
tvp(s)          vtd(RPM)
****************Sinusoidal Disk Flutter*******************
iflut           tsft            teft            fqft            amft
0               0               0.003           10000.0         10.0e-9
*******************Asperity Contact*********************
icmod           ey              ydst            pratio          frcoe
1               9.0e+11         1.0e+10         0.3             0.5
ncz
0
sikm(m)         ceta(/m/m)      rasper(m)       rcts(m)         rcte(m)         glidh
8.0e-9          2.0e+11         1.0e-6          10.0e-3         60.0e-3         10e-9
**********************End of Input Data*******************
```

For the simulation of baseline wander with a single asperity, set *nasper* to be 1. And *iatype, aamp, aang, alocx, alocy, asizx, asizy* correspond to asperity shape, height, orientation angle, location and size respectively. The asperity height can be in the range of 1 ~ 2 times the amplitude of nominal flying height at the central trailing edge. Figure 1 shows an example case for the dynamic simulation of baseline wander. Figure 1 (a) is the rail shape used for this simulation. Figure 1(b) is the time dependent MR temperature and the air bearing spacing at the location of the MR sensor. The size of the asperity used in this case is 40 nm high, 80 μm long and 200 μm wide. In the calculation here, the modified heat flux expression is used (CML Report No. 99-026). This results in the difference between Fig. 1(b) in this report and Figure 7 in CML Technical Report No. 99-06.

It is shown in the figure that the MR temperature fluctuates following the same trend as the air bearing spacing. In the spacing history, the valley with a minimum spacing of about 5 nm corresponds to the spacing when the slider just passes over the asperity. At this moment, the slider is near contact with the disk, and much more heat is transferred from the MR sensor to the disk, so there is a simultaneous drop in the MR temperature. This is the most significant phenomenon when the slider passes over an asperity without contact.

4.3.2. Dynamic response of the slider flying over an asperity with contact (thermal asperity).

Since the contact process is very complicated, there have been quite a few models for calculating the contact force. In our research, we have examined three ways for doing this.

(i) Assuming continuous contact.

In this study, we simplify the case by assuming that the slider is in continuous contact while gliding over the asperity. We also assume that the contact force is uniform and the normal stress equals the yield strength. Therefore the heat per unit area caused by friction is: $q=fv\sigma$, where f is the friction coefficient, v is the velocity, and σ is mean normal stress. We assume that the heat caused by friction diffuses into the slider and the asperity, according to the ratio of their heat conduction coefficients, as obtained by Cook and Bhushan (1973).

The source code for this simulation is *ht3dct.f*. The input file *dynamics.def* is the same as when there is no asperity. The effect of the continuous contact is regarded as a moving heat source with constant speed and area. This part of the simulation is mainly done in *subroutine coef_mtr*. The simulation results for an example case are shown in Figure 8 in CML Technical Report No. 99-06.

(ii) Elastic-plastic model

Set *icmod* in *dynamics.def* to be 2 when the elastic-plastic model is used. When using this model, the slider asperity contact can not be continuous (Hu, Y., 1996). There may be contact at one time step, and then the slider will bounce up but of contact at the next one or two time step. So the difficulty for this study is that very little contact occurs at the MR sensor, and accordingly no MR temperature change is caused by contact friction. And this is not quite consistent with experiments. Quite a few cases have been simulated, and for most of them, the contact point is not at the MR sensor.

Figure 2 shows that the time of the valley of the flying height at the MR sensor is different from the time of contact in the slider history. Figure 2 (a) is the gap spacing and contact pressure for the whole simulation history. Figure 2(b) is the extended plot. We see that contact occurs at about 129 μs after the start of the simulation, while the valley of the gap spacing shows the MR sensor is on the asperity at 135 μs after the starting point. Also the contact time is less than 2 μs. When the disk velocity is around 15 m/s, the contact area has a diameter of only about 30 μm. For a 2 mm long slider, the contact length is about 1.5% of the slider length. Many cases have been studied using different asperity heights, composite elastic modulus and yield stength (*ey* and *ydst* in *dynamics.def*). It's worth mentioning that when *ey* and *ydst* are set smaller, the contact time will be longer due to lower elasticity. For almost all cases that have been studied, the result is similar to that in Fig. 2. Fortunately, there is still one case with contact occurring at the MR element. In this case, the nominal flying height of the tri-pad slider is 39nm and the asperity height is 40 nm. The results of the MR temperature and gap spacing are plotted in Fig. 3. Due to the short contact time, the first peak of the MR temperature, which is caused by contact friction, is also very short. And the following peaks are caused by gap spacing fluctuation.

iii) Greenwood-Williamson Model

Set *icmod* in *dynamics.def* to be 1 when the GW model is used. When the GW model is used, it's assumed that there is a statistical distribution of asperities with different heights on the disk surface. Also set *nasper* to be 1, and set *iatype, aamp, aang, alocx, alocy, asizx* to be the real asperity parameters. When *sikm* (the composite standard deviation for the asperity heights) is set to zero, the disk surface condition is close to smooh except at the real asperity. But when *sikm=0*, it's also hard to catch the contact. In our simulation, *sikm* is set at 8 nm. For this kind of simulation, the contact time can last more than 10 μs, so the contact can occur at the MR element with higher probability. Figure 4 shows the typical response of contact pressure and MR temperature rise using the GW model.

It's worth noting that when the gliding height (*glidh* in *dynamics.def*) is different, the results will be quite different. The gliding height for Fig. 4 is 30 nm, and the gliding height for Fig.5 is 20 nm. When the gliding height is smaller, the calculated contact pressure is smaller, as is the temperature rise.

When the asperity shape is different, the response will also be different. For example, the simulation with an ellipsoidal asperity of 60 nm height and 25 μm in the x and y directions gives the results of MR response similar to those in Figs. 4 and 5, but for a rectangular asperity with the same sizes, the response is very different. The results of gap spacing and MR temperature rise for the rectangular case are plotted in Fig. 6. When the slider flies over the asperity, it goes up dramatically and the gap spacing increases to 200nm. This causes much less heat to be transferred from the slider to the disk, and leads to a temperature increase of several degrees even though there is no contact.

Two kinds of rail designs are also considered to reduce the thermal asperity event. They are shown in Fig.7 (a) and (b). For the convex design, the MR element is after the convex part, and it's assumed that the convex region will reduce the contact chance at the MR element; for the concave design, the MR element is inside the concave region. The GW contact model is used to study several cases of the two designs, but the results didn't show much advantage of these two designs.

5. Subroutine Specification for Thermal Simulation.

datainp: input data from *unstead1.dat, rail.dat, run.dat, x.dat, y.dat* etc.

dataout (key): output data to different files according to the value of key.

grids: generate 3-d grids in the slider body.

starts: set the initial optimized temperature field in the slider body.

unsteady: calculate average temperature, spacing at the MR sensor and output these values to *temp_res.dat*.

matr_sov: solve temperature field in the slider body at each time step, using TDMA method.

coef_mtr: generate the coefficient matrix for each grid in the slider at each time step.

coef_ht (i ,j, sc, sp): calculate heatflux in the air bearing at position (*x(i), y(j))*. The sc and sp are results used for coefficient calculation in *coef_mtr* and *coef_str*.

spacing(x,y,height,press,pct): calculate spacing, pressure, and contact pressure at any position (*x*,*y*).

pgrad(x, y, pgx, pgy): calculate pressure gradient in x and y directions at any position (*x*,*y*).

matr_str: solve static temperature field in the slider body using TDMA method.

coef_str: generate the coefficient matrix for each grid in the slider for static calculation.

6. Some important variables used in the thermal simulation.

xref( ), yref( ) : adaptive grids at the air bearing surface in *x* and *y* directions obtained by CML Air Bearing Dynamic Simulator or CML Air Bearing Design Program.

nx_old, ny_old: grid number corresponding to *xref(i), yref(j).*

xpref( ), ypref( ), zref( ):	grids in the slider body in *x, y* and *z* directions. These grids are generated to accommodate the shape and size of the MR sensor.
nx, ny, nz :	grid number corresponding to *xpref(i), ypref(j), zref(k).*
p(300, 300), pc(300, 300):	normal pressure and contact pressure in air bearing.
q0:	heat generated in the MR element .
xsensl, xsensh :	*x* coordinates of the boundary of the MR sensor (please note the difference between MR element and MR sensor. Refer to Fig. 2 in CML Technical Report 9906).
ysensl, ysensh:	*y* coordinates of the boundary of the MR sensor.
zsensl, zsensh:	z coordinates of the boundary of the MR sensor.
isensl, jsensh:	grid numbers corresponding to *xsensl, xsensh*.
jsensl, jsensh:	grid numbers corresponding to *ysensl, ysensh*.
ksensl, ksensh:	grid numbers corresponding to *zsensl, zsenh*.

References

Burgdorfer, A., (1959), “The Influence of the Molecular Mean Free Path on the Performance of Hydrodynamic Gas Lubricated Bearings”, *J. of Basic Engr.*, Vol. 81, pp.94 100.

Chen, Li and Bogy, D. B., (1999), “A Study of the Thermal Dependence of the MR Signal on Slider Flying State Using a Modified Heat Transfer Model in the Air Bearing”, *CML Report No. 99-026*, Department of Mechanical Engineering, University of California at Berkeley.

Cook, N. H. and Bhushan, B., (1973), “Sliding Surface Interface Temperatures”, *Journal of Lubrication Technology*, Vol. 95, pp.59-64.

Guthrie, A., and Wakerling, R. K., (1949), *Vacuum Equipment and Techniques*, McGraw-Hill Book Company, Inc., New York and London.

Hu,Y. and Bogy, D. B., (1995), “The CML Air Bearing Dynamic Simulator”, *CML report*, *No. 95-001*, Department of Mechanical Engineering, University of California at Berkeley.

Hu, Y., (1996), “Head-Disk-Suspension Dynamics”, *Doctoral Dissertation*, Department of Mechanical Engineering, University of California at Berkeley.

Hu, Y., and Bogy, D. B., (1997), “Dynamic Stability and Spacing Modulation of Sub-25 nm Fly Height Sliders”, *ASME Journal of Tribology*, Vol.119, pp646-652.

Lu, S. and Bogy, D. B., (1995), “CML Air Bearing Design Program User’s Manual”, *CML report*, *No. 95-003*, Department of Mechanical Engineering, University of California at Berkeley.

Lu, S., (1997), Numerical Simulation of Slider Air Bearing, *Doctoral Dissertation*, Department of Mechanical Engineering, University of California, Berkeley.

Mitsuya, Y., (1993), “Modified Reynolds Equation for Ultra-Thin Film Gas Lubrication Using 1.5-Order Slip-Flow Model and Considering Surface Accommodation Coefficient”, *ASME Journal of Tribology*, Vol. 115, pp. 289-294.

Schreck, E., Kimball, R. and Sonnerfeld, R., (1998), “Magnetic Readback Microscopy Applied to Laser-Texture Characterization in Standard Desktop Disk Drives”, *IEEE Transactions on Magnetics*, Vol. 34, No.4, pp1777-1779.

Stupp, S., McEwen, P., and Boldwinson, M., (1998), “Thermal Asperity Model Shows Growing Threat”, *Data Storage*, pp31-32.

Tian, H., Cheung, C-Y., and Wang, P-K., (1997), “Non-Contact Induced Thermal Disturbance of MR Head Signals”, *IEEE Transactions on Magnetics*, Vol.33, No.5, pp3130-3132.

Zhang, S. and Bogy, D. B., (1997), “A Heat Transfer Model for Thermal Fluctuation in a Thin Air Bearing”, *International Journal of Heat and Mass Transfer,*Vol.42, pp1791 -1800.

Zhang, S., and Bogy, D. B., (1998)a, “Variation of the Heat Flux between a Slider and the Air Bearing when the Slider Flies over an Asperity”, *IEEE Transactions on Magnetics*, Vol. 34, No.4, pp1705-1707.

Zhang, S., and Bogy, D. B., (1998)b, “Temperature Response of a MR Head When it Flies Over an Asperity”, *CML report*, *No. 98-001*, Department of Mechanical Engineering, University of California at Berkeley.

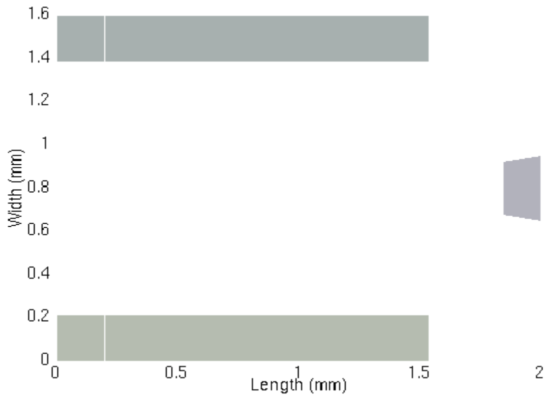

Fig. 1(a) Tri-pad Rail shape

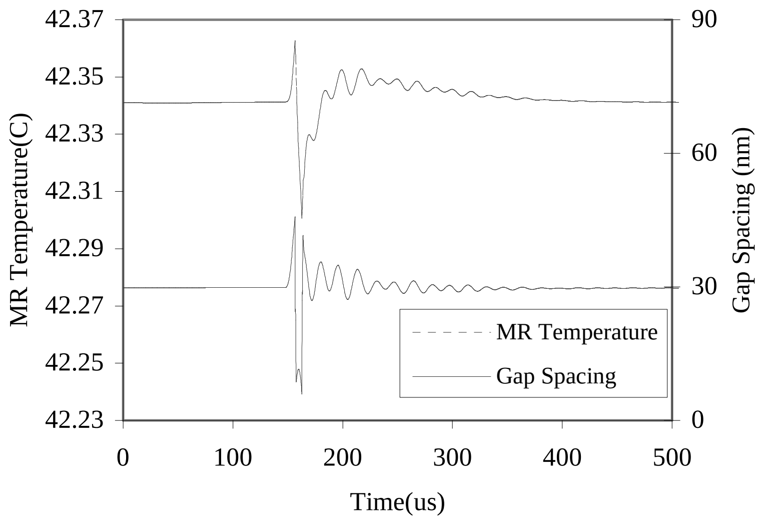

(b)

Fig. 1(b)MR temperature response when slider flies over an asperity wit hout contact

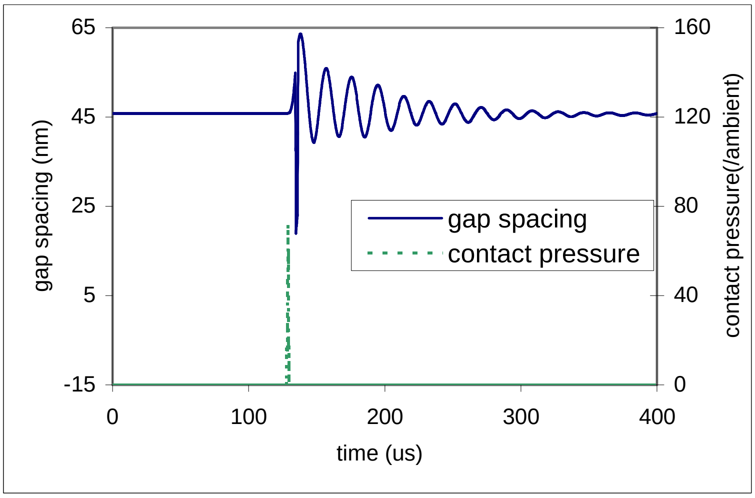

(a)

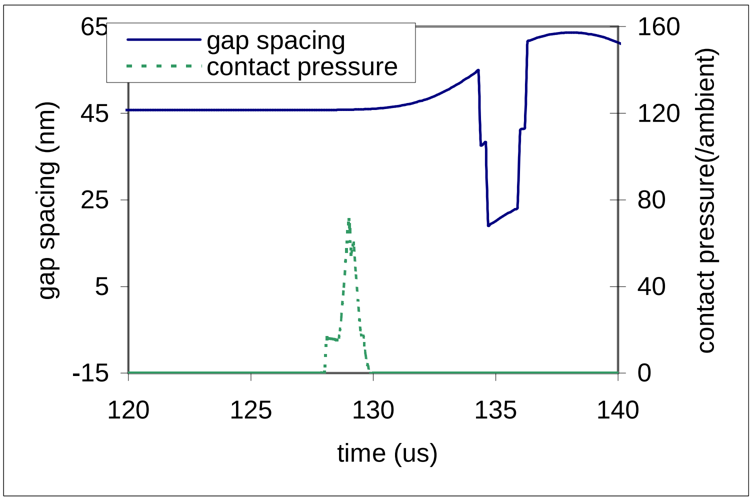

(b)

Fig. 2 Gap spacing and contact pressure versus time when elastic-plastic model is used: (a) for whole simulation time history, (b) extended plot

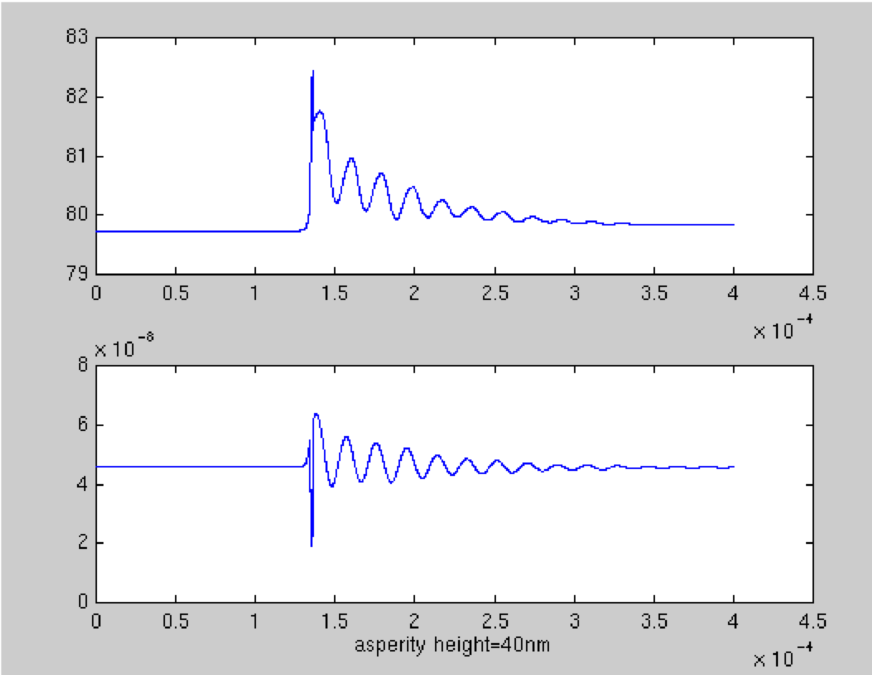

Fig. 3 Results of a contact process using elastic-plastic model: Upper: MR temperature; Lower: gap spacing.

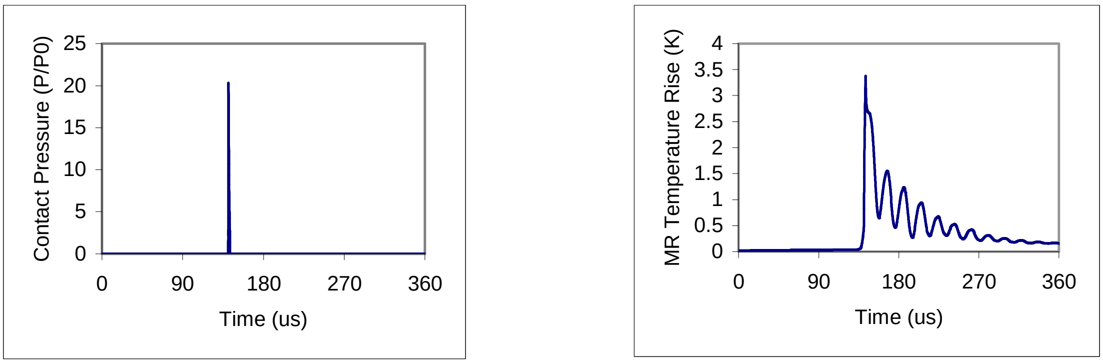

Fig. 4 Simulation results of a contact process using GW model (gliding height = 30 nm): (a) contact pressure at the MR sensor; (b) contact temperature in the MR sensor

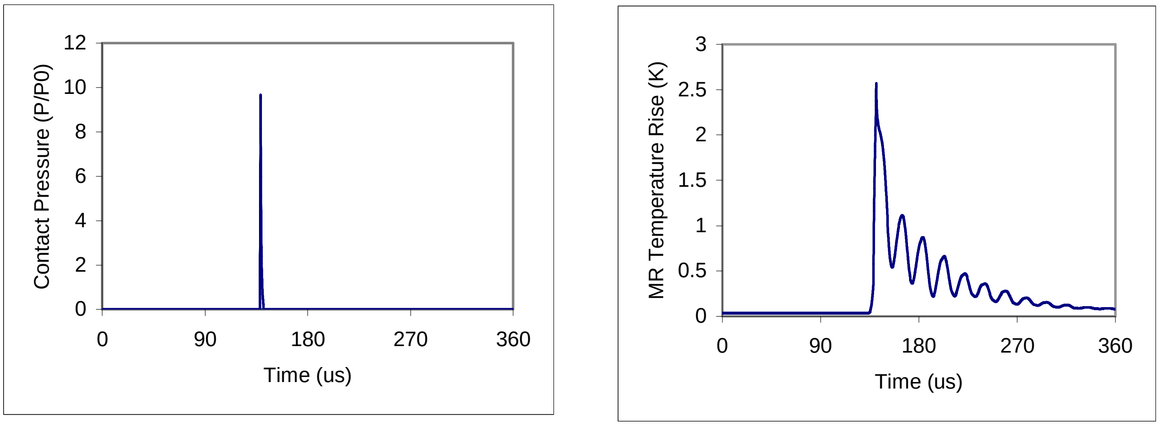

(a) (b)

Fig. 5 Simulation results of a contact process using GW model (gliding height = 20 nm): (a) contact pressure at the MR sensor; (b) contact temperature in the MR sensor

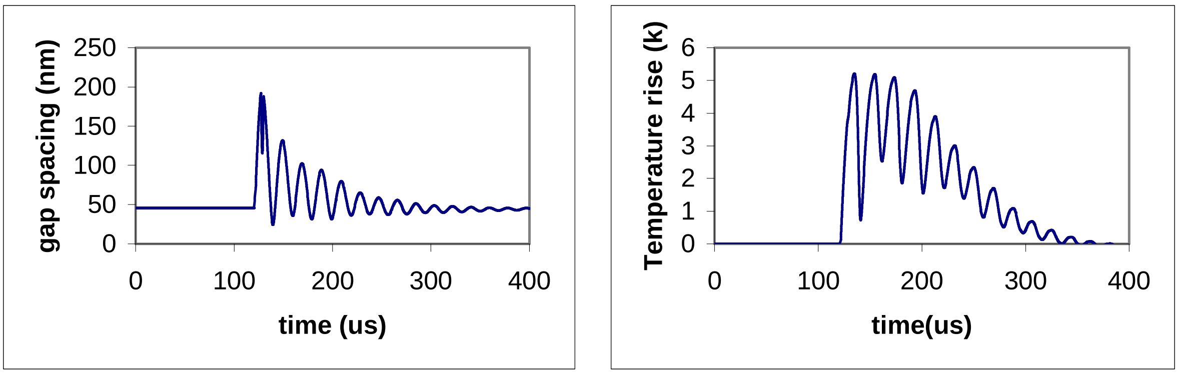

(a) (b)

Fig. 6 Simulation results for a rectangular asperity : (a) gap spacing; (b) temperature rise in the MR sensor.

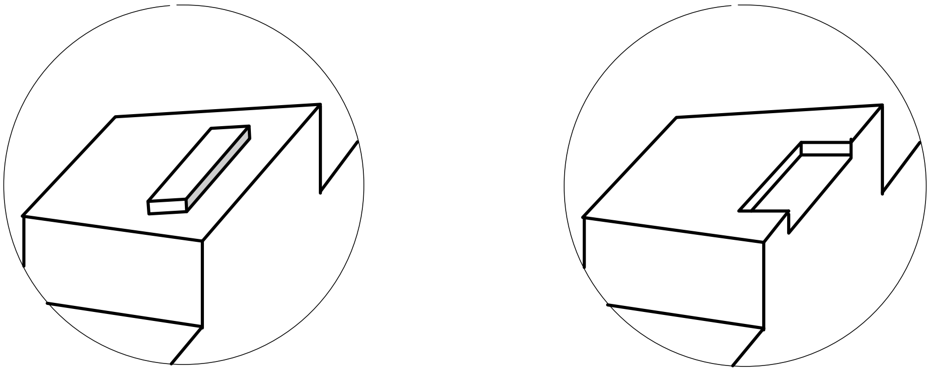

(a) (b)

Fig. 7 Anti-TA design: (a) convex type, (b) concave type